Langmuir

Article

pubs.acs.org/Langmuir

# Polar Solvents Trigger Formation of Reverse Micelles

Atefeh Khoshnood[†] and Abbas Firoozabadi*[,†,‡]

[†]Reservoir Engineering Research Institute, Palo Alto, California 94301, United States

[‡]Department of Chemical and Environmental Engineering, Yale University, New Haven, Connecticut 06510, United States

**ABSTRACT:** We use molecular dynamics simulations and molecular thermodynamics to investigate the formation of reverse micelles in a system of surfactants and nonpolar solvents. Since the early observation of reverse micelles, the question has been whether the existence of polar solvent molecules such as water is the driving force for the formation of reverse micelles in nonpolar solvents. In this work, we use a simple coarse-grained model of surfactants and solvents to show that a small number of polar solvent molecules triggers the formation of large permanent aggregates. In the absence of polar molecules, both the thermodynamic model and molecular simulations show that small aggregates are more populated in the solution and larger ones are less frequent as the system evolves over time. The size and shape of reverse micelles depend on the size of the polar core: the shape is spherical for a large core and ellipsoidal for a smaller one. Using the coarse-grained model, we also investigate the effect of temperature and surfactant tail length. Our results reveal that the number of surfactant molecules in the micelle decreases as the temperature increases, but the average diameter does not change because the size of the polar core remains invariant. A reverse micelle with small polar core attracts fewer surfactants when the tail is long. The uptake of solvent particles by a micelle of longer surfactant tail is less than shorter ones when the polar solvent particles are initially distributed randomly.

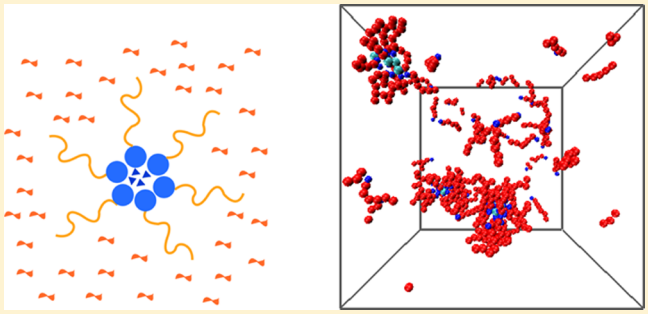

## INTRODUCTION

Micelle structures with definite critical micelle concentration (CMC) generally appear in a mixture of a surfactant and a polar molecule. Figure 1a shows the self-assembly of surfactant molecules in a polar solvent such as water. Molecular models that include salt effect have been suggested to fully describe such direct micelles.[1,2] Direct micelles, however, are not the only end products of the self-assembly of surfactants. In a mixture of surfactants, and nonpolar solvents such as alkanes, a reverse micelle (RM) may form. Figure 1b,c displays a sketch of an RM. Figure 1c is a more realistic representation of an RM, which has trapped polar solvents within its core. In fact, it is widely believed that a small number of polar molecules, such as water, are required in the formation of RMs. Without a limited number of polar molecules, an RM may not form when the surfactant and nonpolar molecules are mixed.[3] The modeling of reversible micelles in multicomponent solvents is a formidable task. This work intends to investigate molecular modeling of RM formation.

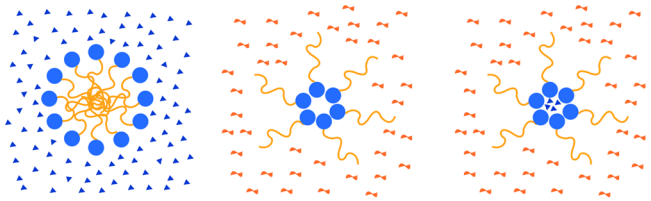


**Figure 1.** Schematics of regular micelle in polar solvent (a), reverse micelle in nonpolar solvent without (b) and with (c) polar solvent in the core.

RMs have enormous applications in technology and sciences. In nanotechnology, the controllable volume within the core of an RM is a reaction medium for the synthesis of nanoparticles.[4] The size of the produced nanoparticles by this method depends on the amount of polar solvents. In biotechnology, where polar macromolecules are not soluble in organic phase, RMs are formed by the addition of surfactants containing polar molecules in their cores and shielding them from external nonpolar media. Protein extraction from aqueous solutions with the help of RMs is an example of solubilizing a polar structure in an organic solvent.[5] In industry, the onset of charges in nonpolar media may be catastrophic;[6] few studies have shown that adding a surfactant stabilizes the charges by forming RMs.[7] In nonpolar suspensions, RMs can disperse aggregated colloids[8] or make them charged.[9] Another interesting application is change of the physical properties of materials by introducing RMs. For example, the formation of RMs increases the viscosity of supercritical $CO_2$ by 100%.[10] New porous materials have been developed by adding RMs in

**Received:** November 28, 2014
**Revised:** March 6, 2015
**Published:** May 5, 2015





DOI: 10.1021/la504658u
*Langmuir* 2015, 31, 5982−5991

the fabrication process of pressure-sensitive rubbers.[11] Reverse micellar systems have also been used to study properties of confined water which depart from the bulk water. Both experimental techniques[12] and atomistic simulations[13,14] have been applied to study the nanoscale water-filled space.

Despite numerous applications of RMs, the exact structure of the core has remained a mystery. Some experimental studies indicate an effectively zero amount of polar solvent (such as water) in the solution,[5,8,15−19] while few authors report traces of water[20,21] or other polar solvents.[22] The molar ratio of the polar solvent to the surfactant is less than unity, $0 < [\text{polar solvent}]/[\text{surfactant}] < 1$, in the latter studies. Generally, the assumption of water-free solutions is not valid; surfactants are able to hold water in their structures, and there is a measurable solubility of water in nonpolar solvents such as *n*-alkanes,[23] aromatics[24] and asphaltenes.[25] The molecular thermodynamic modeling has also shown that in the absence of a polar solvent, the aggregation number in a nonaqueous solution does not go beyond a very small number of surfactants.[3] Neither experimental data nor molecular models have been applied to shed light on the role of polar molecules in the formation of RMs.

Our main goal in this investigation is to study whether polar solvent molecules are essential to form RMs. We use two approaches: molecular thermodynamics and molecular dynamics simulations, which are discussed briefly in the Methods section. The minimization of the Gibbs free energy reveals large aggregates beyond 10 surfactants will not form in the solution. The molecular dynamics simulations show trace amounts of a polar solvent triggers the formation of RM. The results of both methods are presented in the Results section. We also report on the effect of temperature and surfactant tail length on the cluster size distribution. Observations and discussions on the association mechanism and merging process are the last part of the Results section. Finally, we discuss our findings and compare them to experimental data and atomistic simulations. Our findings shed light on the structure of RMs and their inner core and give a roadmap for atomistic simulations and nanoscale experiments.

## METHODS

**Molecular Dynamics Simulation.** We use a simple coarse-grained model for the system of surfactants, nonpolar and polar solvents. The simulation model was first proposed for studying the self-assembly of surfactants in an aqueous environment.[26] The same model can be applied to nonpolar solvents. The model has been adopted for studies on biomembranes, from the measurement of membrane properties such as interfacial tension,[26−28] diffusion,[29] and intermonolayer friction,[27,28] to the investigation of vesicle formation.[30] The model is too simple to allow for a direct quantitative comparison with experimental data. Nonetheless, the model is self-contained enough and provides an excellent tool for qualitative understanding of self-assembly in a solution of surfactants and solvents.

The model is composed of two types of particles: hydrophobic and hydrophilic. The head of surfactant molecules and polar solvents are made up of one hydrophilic particle, while nonpolar solvent is made of one hydrophobic particle. We use surfactants with 4 and 6 hydrophobic particles in their tails − $ht_4$ and $ht_6$, respectively. We use $ht_4$ surfactants in our simulations unless otherwise stated. In surfactant molecules, the head and tail particles are connected to form a chain by a harmonic bond potential, $U_{\text{bond}} = k_{\text{bond}}(r_{ij} - \sigma_{eq})^2$, where $r_{ij}$ is the distance between two particles and $k_{\text{bond}} = 5000\ \epsilon\sigma^{-2}$ is the stretching modulus of the bond. The parameters $\sigma$ and $\epsilon$ are the length and energy scales in our simulations. For surfactant molecules, the equilibrium length of the bonds, $\sigma_{\text{eq}}$ is equal to $1.0\ \sigma$.

A bending potential is used to restrict the flexibility of the surfactant molecule. The bending potential has the form $U_{\text{bend}} = k_{\text{bend}}(1 - \cos\phi_i)$, where $k_{\text{bend}}$ is the bending modulus and $\phi_i$ is the tilt angle between two consecutive bonds. Our results are for simulations with $k_{\text{bend}} = 2\epsilon$; however, we have simulated one case with $k_{\text{bend}} = 0$ as a comparison between a flexible and semiflexible surfactant chain.

The interaction between hydrophobic and hydrophilic particles is modeled through the soft-core potential, $U_{\text{SC}} = 4\epsilon(\sigma_{\text{SC}}/r_{ij})^9$. All other interactions are modeled through the Lennard-Jounes potential, $U_{\text{LJ}} = 4\epsilon((\sigma_{\text{LJ}}/r_{ij})^{12} - (\sigma_{\text{LJ}}/r_{ij})^6)$, where $\sigma_{\text{LJ}} = 1.0\ \sigma$. For both potentials, we use the same cutoff radius, $r_{\text{cut}} = 2.5\ \sigma$. The parameter $\sigma_{\text{SC}}$ is $1.05\sigma$ because the repulsive parts of the soft-core and the Lennard-Jones potentials have the same strength. More details of the model and potential functions can be found in refs 26 and 28.

We use an *NVT* ensemble for molecular dynamics simulations, where the total number of particles $N$, the simulation box volume $V$, and temperature $T$ are constant. The temperature is kept constant using a Nosé−Hoover thermostat. The simulation box is cubic with a length determined by the total number of particles and a constant particle density of $2/3\sigma^3$ that we use for all simulations. The total number of particles and number of each species in the solution are related through $N = N_{\text{W}} + N_{\text{O}} + n_{\text{S}}N_{\text{S}}$, where $n_{\text{S}}$ is the number of particles, either 5 or 7, in a surfactant molecule. The time step for integrating the equations of motion is $0.005\tau$ where $\tau$ is the intrinsic time scale in our simulations. $\tau$ is related to other molecular dynamics scales through $\tau = (m\sigma^2/\epsilon)^{1/2}$, where $m$ is the mass of each particle. All simulations are run over $20 \times 10^6$ time steps corresponding to $t = 10^5\tau$. Boundary conditions are periodic in all directions. Particles are placed initially on a lattice, and we do all measurements after a primary 1000-step simulation to exclude the nonrandom initial positions.

In this work, we do not quantitatively compare our findings with real systems. Therefore, all quantities are presented in molecular dynamics scales, $\epsilon$, $\sigma$, $m$, and $\tau$. To obtain the actual value of any quantity, one can use the following scaling factors: $\sigma = 1/3$ nm, $N_{\text{Av}}\epsilon = 2$ kJ/mol and $N_{\text{Av}}m = 36$ g/mol, where $N_{\text{Av}}$ is the Avogadro number. This set of values for $\sigma$, $\epsilon$, and $m$ set the time scale to $\tau = 1.4$ ps.

**Thermodynamic Model.** The thermodynamic model is based on the work by Ruckenstein and Nagarajan,[3] which uses the multiple equilibrium model of Muller[31,32] for interactions between the head groups of surfactant molecules. However, our model differs from the one in ref 3; we allow for the mixing of nonpolar solvent and surfactant tail in the hydrocarbon layer of an RM. The minimization of the Gibbs free energy of the system provides the equilibrium composition and size of the RM in the solution. The first step is to develop an expression for the Gibbs free energy. The system is composed of two types of molecules: nonpolar solvent and surfactant molecules. The temperature $T$, pressure $p$ and total number of solvent $N_{\text{O}}$ and surfactant $N_{\text{S}}$ molecules are constant. The Gibbs free energy of the system thus reads



DOI: 10.1021/la504658u
Langmuir 2015, 31, 5982−5991

$$G = G_f + G_m + G_i \quad (1)$$

where $G_f$ and $G_m$ are, respectively, the free energies of the formation and mixing in the solution. The free energy of interactions between micelles, can be neglected, $G_i \approx 0$, if one assumes a dilute system. The formation energy is given by

$$G_f = N_{1O}\mu_O^\circ(T, p) + N_{1S}\mu_{1S}(T, p) + N_g\mu_g(T, p) \quad (2)$$

When an RM is formed, some solvent molecules move to the hydrocarbon layer of the micelle and become part of the micelle as seen in Figure 1c. As pointed out above, this is a more complete formulation than the model in ref 3. A micelle may have solvent molecules in its structure. In eq 2, $N_{1O}$ and $N_{1S}$ are, respectively, the number of solvent and surfactant molecules that are free in the solution and are not part of an RM. $N_g$ is the number of RMs. In eq 2, $\mu_O^\circ$ is the standard state chemical potential of the solvent, and $\mu_{1S}$ is the chemical potential for singly dispersed surfactant in the solution. $\mu_g$ is the chemical potential for a micelle in the solution. Note that we assume the micellar system to be a monodispersed solution with RMs of the size $g$ where $g = g_S + g_O$, and $g_S$ and $g_O$ are the number of surfactant and solvent molecules in an RM, respectively. The monodispersity assumption is reasonable because there are experimental evidence showing such systems have RMs of uniform size, and the size does not change with increasing number of surfactant molecules in the system.[21,33] The mass balance equations of species are

$$N_O = N_{1O} + g_O N_g \quad (3)$$

and

$$N_S = N_{1S} + g_S N_g \quad (4)$$

The free energy of mixing in the solution is

$$G_m = k_B T[N_{1O} \ln X_{1O} + N_{1S} \ln X_{1S} + N_g \ln X_g] \quad (5)$$

where $k_B$ is the Boltzmann constant, and we have

$$X_{1O} = \frac{N_{1O}}{N_{1O} + N_{1S} + N_g} \quad (6)$$

$$X_{1S} = \frac{N_{1S}}{N_{1O} + N_{1S} + N_g} \quad (7)$$

and

$$X_g = \frac{N_g}{N_{1O} + N_{1S} + N_g} \quad (8)$$

In our formulation of reverse micellar systems, the total Gibbs free energy is a function of $T$, $p$, $N_O$, $N_S$, $N_g$, $g_O$, and $g_S$. The independent variables $N_g$, $g_O$, and $g_S$ define the system. We collect the terms of $G$ that depend only on the fixed variables, and introduce

$$G' = G - N_O\mu_O^\circ - N_S\mu_{1S} \quad (9)$$

By substituting from eqs 5 and 2 into eq 1, and using the result to simplify eq 9, we arrive at

$$G' = g_S N_g \Delta\mu_g^* + k_B T[N_{1O} \ln X_{1O} + N_{1S} \ln X_{1S} + N_g \ln X_g] \quad (10)$$

where

$$\Delta\mu_g^* = \frac{1}{g_S}\mu_g - \mu_{1S} - \frac{g_O}{g_S}\mu_O^\circ \quad (11)$$

is the free energy change due to the transfer of one surfactant molecule at infinite dilution from the nonpolar environment, and $g_O/g_S$ are solvent molecules from the pure state to the RM. The free energy of micellization $\Delta\mu_g^*$ can be split into contributions from different energies:

$$\Delta\mu_g^* = (\Delta\mu_g^*)_{\text{dipole-dipole}} + (\Delta\mu_g^*)_{\text{trans}} + (\Delta\mu_g^*)_{\text{mix}} \quad (12)$$

Later in this section, we will discuss how to calculate each term; the energy of dipole−dipole interaction, $(\Delta\mu_g^*)_{\text{dipole-dipole}}$, the energy due to loss of translational motion of surfactant, $(\Delta\mu_g^*)_{\text{trans}}$ and the energy related to mixing of oil molecules and surfactant tails in the hydrocarbon layer of an RM, $(\Delta\mu_g^*)_{\text{mix}}$. The free energy of a system with no micelles has only the terms from mixing. One thus obtains

$$G' = k_B T\left[N_{1O} \ln \frac{N_{1O}}{N_{1O} + N_{1S}} + N_{1S} \ln \frac{N_{1S}}{N_{1O} + N_{1S}}\right] \quad (13)$$

*Free Energy of Reverse Micelle Formation.* The important term in the Gibbs free energy of a micellar system is the formation free energy, which includes terms from driving and restrictive energies. We consider dipole−dipole interactions between surfactant heads as the driving energy for the formation of RMs as suggested in ref 3. In both ionic and nonionic surfactants, the headgroup is polar. For an ionic surfactant in a nonpolar solvent, the counterion, which always dissociates in aqueous solutions, stays in the headgroup and forms a dipole in the head of the surfactant. This dipole has electrostatic interactions with dipoles of other surfactant heads. The first effort in calculating dipole−dipole interactions for RMs was by Muller,[31,32] who studied the formation of RMs by considering electrostatic forces alone. He calculated dipole−dipole interactions for a cluster of 2, 3, and 4 surfactants and then built larger aggregates by combining smaller ones. This strategy gives ellipsoidal RMs for large aggregation numbers. The free energy change of the dipole−dipole interactions can be obtained from

$$(\Delta\mu_g^*)_{\text{dipole-dipole}} = -\frac{e^2}{Dd}\left[\frac{[0.75/(\delta/d) - 0.33](g_S - 1)}{[0.2(\delta/d) + g_S]}\right] \quad (14)$$

where $e$ is the charge of an electron, and $D$ is the dielectric constant of the solvent medium. If the positive and negative partial charges in the surfactant be charge points, $d$ will be the distance between them. Thus, $\delta$ becomes the distance between two neighboring dipoles within the core of the RM.

The dipole−dipole interaction can drive the formation of RM. The loss of translational motion limits the growth of micelles; singly dispersed monomers freely translate in the solution, while the surfactants in an RM have restricted translational motion. The energy related to this loss can be calculated through[3]



DOI: 10.1021/la504658u
Langmuir 2015, 31, 5982−5991

$$(\Delta\mu_g^*)_{trans} = -\frac{k_BT}{g_S}\left\{\ln\left[\left(\frac{2\pi M g_S k_BT}{h^2}\right)^{3/2} v_O f_1\right] + (g_S - 1)\ln\left[\left(\frac{2\pi M k_BT}{h^2}\right)^{3/2} V_{acc} f_2\left(\frac{V_{acc} - g_S v_0}{V_{acc}}\right)\right] - \ln g_S! - g_S \ln\left[\left(\frac{2\pi M g_S k_BT}{h^2}\right)^{3/2} v_O f_1\right]\right\} \quad (15)$$

The details of obtaining $(\Delta\mu_g^*)_{trans}$ are presented in ref 3. There are many parameters in the calculation of $(\Delta\mu_g^*)_{trans}$ that should be estimated from experimental data. In eq 15, $M$ is the mass of the surfactant molecule, and $h$ is Planck's constant. The parameter $f_1$ is the free volume fraction of the solvent. It is estimated from[34]

$$f_1 = \frac{4\pi}{3v_O}\left(\frac{v_O - v_{VWO}}{A_{VWO}}\right)^3 \quad (16)$$

where $v_{VWO}$ and $A_{VWO}$ are the van der Waals volume and area of the nonpolar solvent molecule. We can estimate the accessible volume $V_{acc}$ for the tails of surfactant molecules from

$$V_{acc} = 2(g_S^{1/2} - 1)^2\delta^2 l_{St} + 2(g_S^{1/2} - 1)\pi\delta l_{St}^2 + \frac{4}{3}\pi l_{St}^3 \quad (17)$$

by assuming an elongated disk shape for an RM. The first term accounts for two flattened volumes perpendicular to the surface of surfactant heads. The second term represents the four sides hemicylinders, and the third term is the left volume at the four corners, each approximated by a quarter of a sphere. $l_{St}$ is the surfactant tail length. Similar to $f_1$, $f_2$ is the free volume fraction of a fluid composed of the hydrocarbon tails of the surfactant, and is estimated by an equation similar to eq 16.

The tails of the surfactants and solvent molecules mix in the hydrophobic layer of the RM. The free energy change of mixing is estimated by the Flory–Huggins expression:

$$(\Delta\mu_g^*)_{mix} = k_BT \ln\eta_S + k_BT\frac{g_O}{g_S}\ln\eta_O + v_{St}(\delta_S^H - \delta_{mix}^H)^2 + v_O\frac{g_O}{g_S}(\delta_O^H - \delta_{mix}^H)^2 \quad (18)$$

where

$$\eta_S = \frac{v_{St}}{v_{St} + v_O\frac{g_O}{g_S}}, \qquad \eta_O = \frac{v_O\frac{g_O}{g_S}}{v_{St} + v_O\frac{g_O}{g_S}} \quad (19)$$

Here, $v_{St}$ and $v_O$ are the volumes of the surfactant tail and solvent molecules, respectively. Note that $v_{St}$ should be doubled if the surfactant has two tails, or tripled if it has three. In eq 18, the constants $\delta_S^H$ and $\delta_O^H$ are the Hildebrand solubility parameters of the surfactant and solvent molecules, respectively. We have used the solubility values 14.0 $MPa^{1/2}$ and 20.0 $MPa^{1/2}$ for oil and surfactant tails, respectively.[35] The solubility parameter for the mixture of the two species can be calculated using $\delta_{mix}^H = \eta_S\delta_S^H + \eta_O\delta_O^H$. We emphasize that the main difference between the model of ref 3 and ours is that in our work we account for mixing in the hydrocarbon layer of the micelle.

We define $\alpha = g_O/g_S$. Then, the independent variables for minimization of the Gibbs free energy will be $N_g$, $g_S$, and $\alpha$. The new variable $\alpha$ is more convenient for minimization compared to $g_O$ since its upper and lower bounds are clearer. In minimization, we have examined values as large as 3 for the upper bound of $\alpha$. To minimize the total Gibbs free energy, we use the optimization routine FFSQP.[36]

## RESULTS

**Molecular Thermodynamics.** We use the molecular thermodynamic model to investigate the formation of RM in the system of surfactants and nonpolar solvents. We choose isooctane as the nonpolar solvent and sodium dioctylsulfosuccinate (Aerosol OT or AOT) as the surfactant. NaAOT is the commonly used surfactant for RM formation, and there are several experimental measurements of its CMC in a variety of nonpolar solvents.[15,21,37] Reported CMCs are as low as 0.18 mmol $L^{-1}$ in cyclohexane, compared to the CMC of NaAOT in water, which is 6.2 mmol $L^{-1}$. In the minimization of the Gibbs free energy, we use $N_O = 10^8$ and increase the number of surfactant molecules gradually to find if a micelle will form. Following values are used for NaAOT in the thermodynamic model: 0.200 $nm^3$ and 0.236 $nm^3$, for the tail and head volumes, respectively.[38] For the tail, a length of 0.8 nm is used.[20]

The mole fraction of the singly dispersed surfactants versus the total mole fraction of surfactants is plotted in Figure 2.

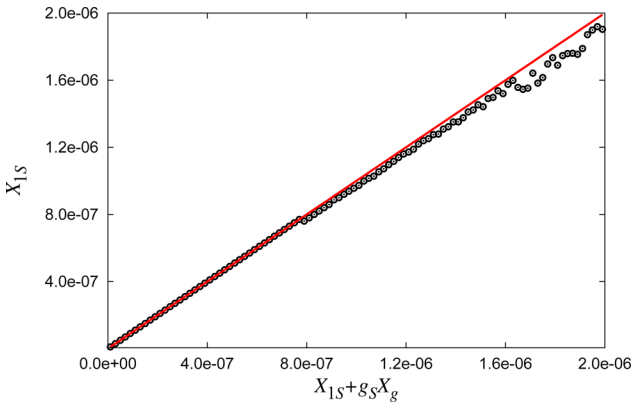


**Figure 2.** Mole fraction of the singly dispersed surfactants versus the mole fraction of the total surfactants in the solution. The solid line has a slope of 1.

Micellization occurs when the slope of the line sharply deviates from unity. At a total mole fraction of $8.2 \times 10^{-7}$, the first aggregate forms. However, the size of the aggregate is $g_S = 3$, which is small and can not be considered as a micelle. By introducing more surfactants to the solution, the numbers of trimers grows, and then $g_S$ increases but does not pass 10. This results in more deviation from the unity slope, as seen in Figure 2 at the total mole fraction $1.6 \times 10^{-6}$. Moreover, the ratio of the nonpolar solvent and surfactant in the aggregates does not go above 0.3, which is effectively zero for aggregates with $g_S <$ 10. Figure 2 implies that there is no clear CMC for a system of surfactant and nonpolar solvent. In a polar solution the main driving force for micelle formation is the free energy of transferring surfactant tails from contact with water to the hydrocarbon core of the micelle. This energy is constant for all aggregate sizes.[39] The free energy of the interface formation between an aqueous medium and hydrocarbon tails contributes to the growth of micelles since it strictly decreases with $g_S$.



DOI: 10.1021/la504658u
Langmuir 2015, 31, 5982−5991

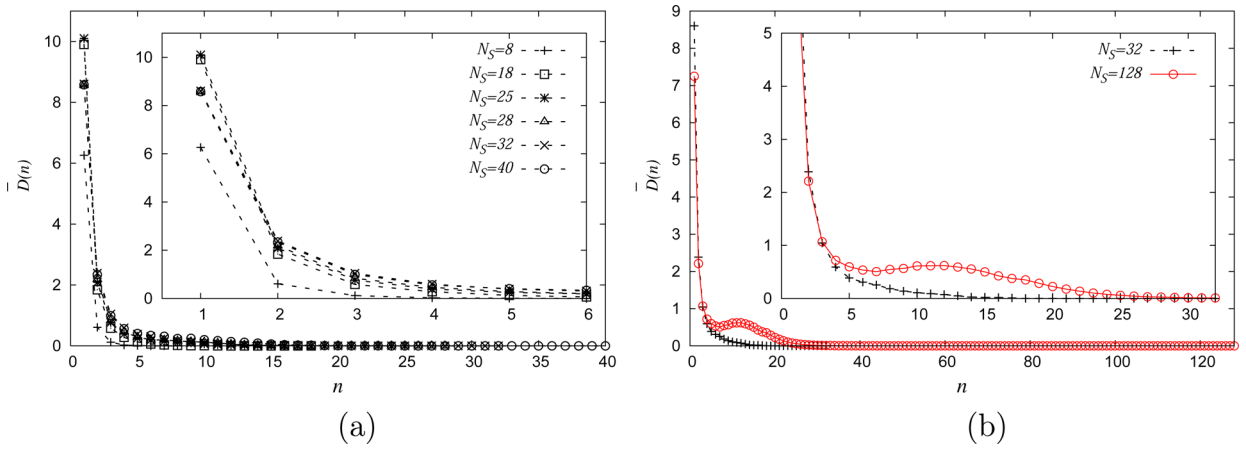


**Figure 3.** Average number of aggregates with $n$ surfactant molecules. (a) The number of surfactant molecules is varied from 8 to 40. (b) Two systems with 128 and 32 surfactant molecules are simulated. In all simulations, there is no polar solvent, the total number of particles is 8000, and averages are computed over a simulation time of $t = 10^5\tau$.

Other contributions like ionic or headgroup steric interactions put a limit on $g_S$ and restrict the micelle size. A basic difference between a regular micelle and a system with nonpolar solvent and surfactant is the absence of interactions needed to boost the formation of large aggregates. Dipole−dipole interaction is the driving force for aggregation in nonpolar media and it is almost constant as the size of aggregates increases. This interaction replaces the role of tail transfer energy in water-based solutions. On the other hand, the loss of translational freedom limits the formation of large aggregates since it increases with $g_S$ for $g_S > 10$. However, there is no energy contribution to play the same role as the energy of interface formation in an aqueous medium.

The thermodynamic modeling provides aggregates with $gs < 10$, while $N_g$ is low with no clear CMC. In the next section, we will use an empirical coarse-grained model of surfactants and solvents to examine whether the sole disaffinity property of oil for polar heads results in RM formation, or there is a need for other driving forces and components.

**Molecular Simulations: Without Polar Solvent.** We first simulate systems containing only surfactants and nonpolar solvents. Starting from a small number of surfactants, we gradually increase the concentration to investigate any threshold for the start of micellization. The total number of particles $N$ is 8000, which is fixed in all simulations with no polar solvent. In all simulations, we observe no growth of aggregates, rather we find a distribution of small-size aggregates that associate and dissociate during the course of simulation. To quantify our observations, we compute the size distribution of aggregates up to $t = 10^5\tau$ by counting the number of surfactants $n$ in each cluster. The cluster size distribution is calculated for every $5\tau$ time step, and then the average is obtained by adding all distributions and dividing by 20 000, which is the total number of studied snapshots. Note that two surfactant molecules are considered to be in the same cluster if their heads are within $4.0\sigma$ of each other. This cutoff radius is large enough to account for any possible aggregation configurations, e.g., two surfactant molecules form a dimer if their heads are close to each other, or one tail particle is close to the head of the other surfactant.

The average number of aggregates with $n$ surfactants, $\bar{D}(n)$, is plotted in Figure 3a. The distribution trend is in agreement with results from the molecular thermodynamic model, which indicates a more frequent occurrence of smaller aggregates in the system. The general form of the distribution does not change by varying $N_S$. When the number of surfactant molecules in the system is 18 and more, there is no appreciable change in $\bar{D}(n)$. We also examine the effect of surfactant chain flexibility. We observe that flexible surfactant chains with $k_b = 0$ show no sign of even temporary aggregation and they stay mostly singly dispersed in the solution. An inspection of the simulation snapshots shows that this happens because the flexible hydrocarbon chain in the tail shields the polar head from the nonpolar solvents by coiling around the head and reducing the contact with solvent.

The molecular thermodynamic model predicts the formation of small aggregates $g_S < 10$ and growth in their density when the concentration of surfactant molecules is very high compared to the measured CMC in RMs (for typical surfactants). The same observation is made in the molecular dynamics simulations. In Figure 3b, we illustrate the average number of aggregates with size $n$ for two systems with large difference in surfactant concentration. The system with higher concentration, $N_S = 128$, develops a peak with its maximum at $n = 12$. The aggregates with $9 < n < 15$ are not spherical; they are more like an elongated disk, as presumed in the molecular thermodynamic model.

**Molecular Simulations: With Polar Solvent.** We examine the system with a small number of polar solvent molecules to see whether permanent large aggregates will form. We simulate a system with $N = 8000$ and 32 surfactant molecules, while increasing $N_W$ from 0 to 32. We discuss the cases that the polar solvents are initially close to each other, and form a single drop at the early stages of the simulation. We find that depending on the size of the polar drop, a permanent structure of surfactants forms around it, and the RM will stay stable throughout the simulation. We quantify this observation by calculating the size distribution of aggregates (see Figure 4). Note that when surfactant heads do not cover the entire surface of the polar drop, a larger radius of $5.0\sigma$ is used (based on visual inspection of RM) to determine whether two surfactants belong to the same cluster. From Figure 4, it is clear that the polar solvent can attract singly dispersed surfactants. As the number of polar solvent molecules increases, the number of monomer surfactants decreases sharply. The average number of monomers is about 9 for $N_W = 0$ and decreases to nearly 3



DOI: 10.1021/la504658u
Langmuir 2015, 31, 5982−5991

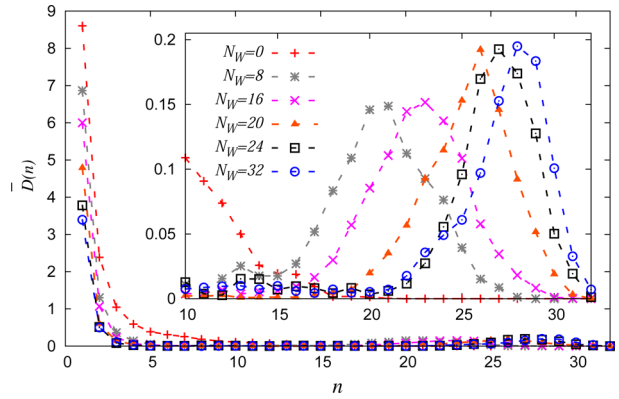


**Figure 4.** Average number of aggregates with $n$ surfactant molecules when polar solvent molecules are added to the system. The inset plot shows that the distributions develop peaks when polar solvents are added. In all simulations we have $N$ = 8000 and $N_S$ = 32, and averages are computed over a simulation time of $t = 10^5\tau$.

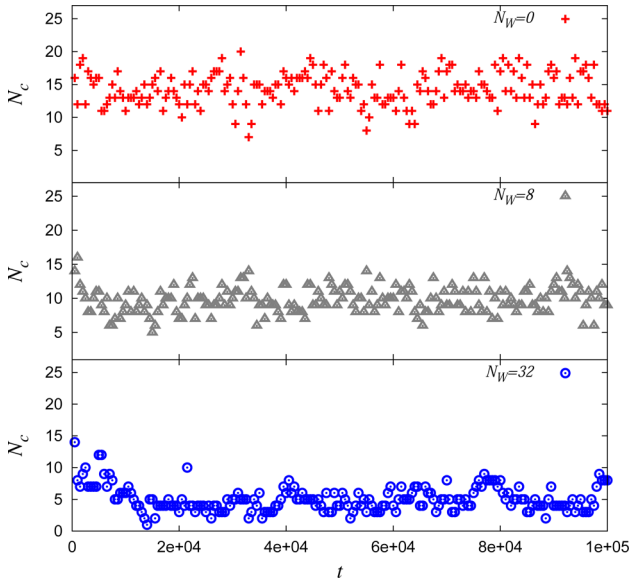


**Figure 5.** Temporal evolution of the total number of aggregates for systems with 0 (top), 8 (middle) and 32 (bottom) polar solvent particles. For all three systems, the total number of particles and number of surfactant molecules are 8000 and 32, respectively.

when 32 polar particles are present in the simulation box. Reduction of singly dispersed surfactants is a sign of micellization, triggered by polar molecules in the solution. The same decrease in average number happens for other small size aggregates ($n$ < 15).

For $N_W$ > 0, each distribution profile in Figure 4 develops a small peak for $n$ > 15. This is a demonstration of micelle formation around the polar drop. We have also performed simulations for systems with 1 and 4 polar solvent particles and 32 surfactants. There is a clear peak at $n$ = 18 for $N_W$ = 4, and therefore, a polar drop consisting of 4 polar particles can lead to micellization, as well. For $N_W$ = 1, there is not a clear preference for a large aggregate size. The number of surfactants contributing to the micelle increases as the size of the polar drop grows (higher $N_W$).

For lower values of $N_W$, like 8 and 16, the number of surfactants in the RM has a larger variation and wider distribution. Increasing $N_W$ gives a narrower distribution. The reason is hidden in the concentration of singly dispersed surfactants, which is higher for smaller $N_W$. This results in higher probability in the exchange of surfactants between the RM and the solution, and hence wider distribution.

Figure 5 illustrates the evolution of the total number of aggregates during the simulation including monomer surfactants as well. There is a clear decline in the total number of aggregates, $N_c$, when polar solvent exists in the solution. The average number of clusters are 14, 10, and 5 for systems with $N_W$ = 0, 8 and 32, respectively. There is a fast initial clustering of surfactants for systems with polar solvents which reduces $N_c$ at $t \approx 10^4\ \tau$. When $N_W$ = 0, the total number of clusters only fluctuates around a mean value, and no decline is observed. The time evolution of the total potential energy of the system, $U_{tot}$, shows the same relaxation time for the fast initial clustering in solutions with polar solvents. In a nonpolar solution, $U_{tot}$ oscillates about a median value and shows no sign of decline/rise.

One basic difference between a regular micelle and an RM is that the physical size of the latter depends on the size of the polar drop rather than the number of surfactants in the micelle. Therefore, any variation in the radius of an RM scales with the size of its polar pool. Increasing temperature may result in smaller cores, and consequently, decreases the radius of an RM. In order to investigate this effect, we perform simulations at a higher temperature of $k_BT = 1.35\epsilon$. Our results, for a system of $N_W$ = 16 and 32 with $N_S$ = 32 and $N$ = 8000, show that the median number of surfactants in an RM decreases at higher temperatures while the size of the polar pool is unaltered compared to the lower temperature simulations. We conclude that the average diameter of an RM does not change with temperature. This is in agreement with experimental measurements.[15] We note that, in a reverse micellar system, the density of hydrogen bonds is very low, and the polar components are not dominant in the solution. Therefore, as long as the added polar solvent molecules are in a trace amount, the predictions of the coarse-grained model on effect of temperature can be trusted.

**Effect of Hydrocarbon Tail Length.** To study the effect of hydrocarbon tail length on RM formation, we simulate systems with surfactant, $ht_6$. Five systems with $N_W$ = 0, 8, 16, 24, and 32 are studied by fixing $N$ = 8000 and $N_S$ = 32. The average number of aggregates for the $ht_6$ surfactant is plotted in Figure 6 together with the results for $ht_4$. The profiles for $N_W$ = 0 are almost identical for $ht_4$ and $ht_6$. This implies that the tail length has no effect on the formation of small-size aggregates, and it does not alter the distribution in the absence of polar molecules. When a polar solvent is added in low amount, e.g., $N_W$ = 8, the average number of surfactants in an RM is higher for $ht_4$ compared to $ht_6$, respectively. The same difference is observed for $N_W$ = 4 (not shown). However, as the size of the polar core increases, the difference becomes small. For example, consider the case of $N_W$ = 32 in Figure 6.

We explain this observation by considering the density of tails in the hydrocarbon interface of an RM. The volume of the interface layer depends on two parameters: the core radius and thickness of the layer, which is a function of the surfactant tail length. When the polar core is small, the interface volume becomes smaller. For a longer surfactant tail, the hydrocarbon layer thus becomes more compact and denser. This will obstruct the head of a new surfactant from reaching the surface of the polar core, and therefore, reduces the number of surfactants in an RM. However, when the core becomes large



DOI: 10.1021/la504658u
Langmuir 2015, 31, 5982−5991

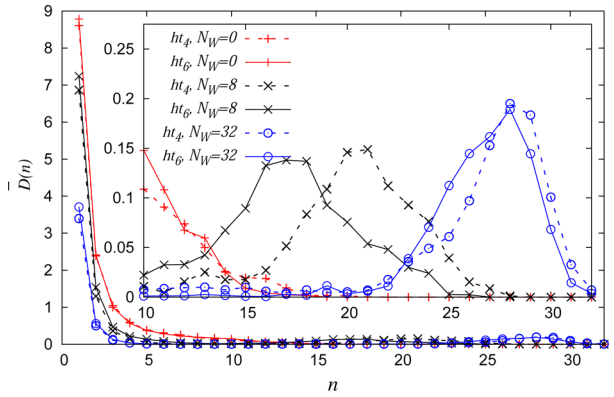


**Figure 6.** Average number of aggregates with $n$ number of surfactant molecules of different tail lengths when the number of polar solvents increases from 0 to 32. Solid lines represent results for the longer tail length. In all simulations we have set $N$ = 8000 and $N_S$ = 32, and averages are computed over a simulation time of $t = 10^5\ \tau$.

compared to the thickness of the layer, the volume of the interface becomes a function of the size of the core rather than the length of the surfactant tail. The density of hydrocarbon tail particles thus decreases in the interface layer, and more surfactant heads may reach the surface of the polar pool.

**Molecular Simulations: Association Mechanism.** We carry out simulations of a system of 27000 total particles, with 50 surfactants and $N_W$ = 100. The polar solvent particles are evenly distributed in the solution initially, to avoid the formation of a single polar drop at the early steps of the simulation. The final state of this set up is a single RM with all polar solvent particles within the core. The initial stages, however, show the mechanism of surfactant association and the process of merging of smaller RMs.

In general, there are two models of multimerization.[40] One model is the closed association in which the dynamic equilibrium exists between $n$ monomers and an aggregate of $n$ molecules. This is also called the mass action model and is broadly accepted for the systems of aqueous solutions like regular micelles.[41] For nonaqueous systems, however, experimental evidence[42] is not in line with the closed association model. The proposed mechanism for such systems is a multiple equilibrium process where the number of surfactants in the micelle grows gradually through a continuous process. Therefore, in the open association scheme, the equilibrium is between monomers, dimers, trimers, etc.

The examination of the simulation box shows an open association mechanism for the formation of RM. The process starts by clustering of polar solvents and the formation of several drops in the nonpolar medium (see Figure 7 left panel). Singly dispersed surfactants then come in contact with the polar drops and their number increases continuously around polar pools until they shield them from the nonpolar solvent (see Figure 7 right panel).

**Merging of Micelles.** In our simulations, with a limited number of surfactant and polar molecules, the final configuration for all systems is a single RM, which is in equilibrium with singly dispersed surfactants and constantly exchanges monomer with the solution. We observe that the smaller size RMs merge during the course of simulations. The merging process is shown for a system containing 27 000 total particles, 50 surfactants, and 100 polar solvent particles in Figure 8. Merging ocurrs when the polar pools at the interior of

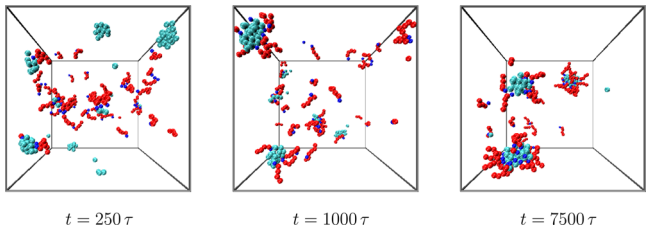


**Figure 7.** Early time snapshots show the formation of small RMs through the open association mechanism. The polar solvent, head and tail of surfactants are presented by cyan, blue, and red spheres, respectively. Nonpolar solvent particles are omitted for clarity. Time increases from left to right, and from top to bottom. The total number of particles in the simulation box is 27000 with $N_S$ = 50 and $N_W$ = 100.

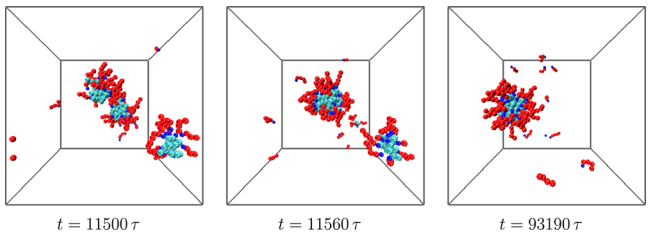


**Figure 8.** Snapshots of the steps in the simulation that two smaller RMs merge through the contact between their polar pools. Polar solvent, head, and tail of surfactants are presented by cyan, blue, and red spheres, respectively. Nonpolar solvent particles are omitted for clarity. The total number of particles in the simulation box is 27000, while $N_S$ = 50 and $N_W$ = 100.

the two micelles are close enough to make contact and form a larger drop. Then the surfactants rearrange themselves around the new polar nucleation site. Observation of the system evolution shows that the contact between the two polar drops triggers the merging and results in a single stable RM. We argue that three parameters control the merging: (1) the thickness of hydrocarbon layer of the RMs, (2) the ratio of the number of polar solvents in the core to the number of surfactants in the RM, and (3) total surfactant concentration.

To examine our argument, we change the original simulation set up ($N$ = 27 000, $N_S$ = 50, and $N_W$ = 100) and run several simulations to investigate the effect of the three parameters mentioned above. In order to change the hydrophobic thickness of RM, we use the surfactant with longer tail $ht_6$ in the simulations. To alter the ratio of polar solvents to surfactants in the RM, we change the concentration of polar solvents in the solution. We also simulate a more concentrated solution of 84 surfactants to study the effect of total surfactant concentration on merging of aggregates.

In all the simulations except one, multiple micelles form; however, they merge during the course of simulation and the final equilibrium state is a single RM in equilibrium with several monomers in the solution. The only system that develops multiple RMs in the stable state is the setup with $N_S$ = 84, $N_W$ = 10, and $ht_6$ surfactant. There are three stable RMs in this system with 2, 4, and 4 polar solvent particles at their cores and average of 13 surfactants shielding the polar pools. The distribution of aggregates for this system is shown in Figure 9a along with the distribution of the same system with $ht_4$ surfactants, which develops a single RM with 10 polar solvent particles in the core. The average number density of RMs is almost 3 times higher in $ht_6$ compared to $ht_4$, which demonstrates the formation of three individual micelles. The last configuration of the system with



DOI: 10.1021/la504658u
Langmuir 2015, 31, 5982−5991

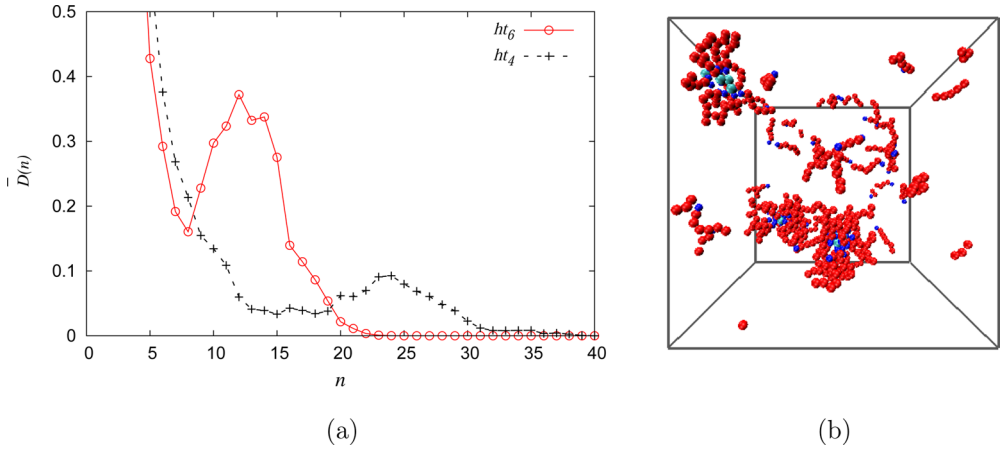


**Figure 9.** (a) Average number of aggregates with $n$ surfactant molecules for systems with $ht_6$ and $ht_4$. The total number of particles in both simulations is 27 000 with $N_S$ = 84 and $N_W$ = 10. Averages are computed over a simulation time of $t = 10^5\tau$. (b) Snapshot of the system with $ht_6$ surfactants from (a) forming three RMs at the end of simulation, $t = 10^5\tau$. Polar solvent, head, and tail of surfactants are presented by cyan, blue, and red spheres, respectively. Nonpolar solvent particles are omitted for clarity.

$ht_6$ surfactants is shown in Figure 9b, where there are three micelles with 4, 2, and 4 polar solvents at their cores.

## DISCUSSIONS AND CONCLUSIONS

Our results clearly demonstrate the role of polar solvents in RM formation. The molecular thermodynamic modeling of a two-component system, oil and surfactant, predicts no clear CMCs and only formation of small-size aggregates, $g_S < 10$. Our coarse-grained simulations verify those results and reveal that the trace amounts of the polar solvent provide nucleation sites, and permanent clusters establish in the solution after adding as few as four polar solvent particles. Therefore, we conclude that the formation of an RM solely depends on the presence of small amounts of polar solvent molecules in the solution.

One question arises: can we compare the results of the two models? We have replaced the attractive dipole−dipole interactions between heads (affinity of polar groups in the thermodynamic model), with repulsive soft-core interactions (disaffinity of polar particles for nonpolar ones and vice versa) in the coarse-grained model. We argue that either of these interactions can, in general, lead to a separation between hydrophobic and hydrophilic particles.[43] A comparison between the size distributions of our molecular simulations in Figure 3b and those of Figure 3 in ref 3 shows their similarity, and further validates the analogy between dipole−dipole interactions and the soft-core potential. Other contributions in the thermodynamic model, such as mixing and loss of translational motion, are included naturally in molecular dynamics simulations.

There are many atomistic simulations of surfactants, polar and nonpolar solvents,[13,33,44,45] and experimental measurements,[33] all dedicated to higher molar ratios of water and surfactants, $w_0$ = [water]/[surfactant] > 1. Almost all simulations start from a preassembled spherical RM with a spherical water pool at the center,[13,44] in which the polar core is constrained to stay in a spherical shell during the simulations. Reference 44 reports a pseudolattice structure of sulfate heads, water molecules, and sodium ions at the surfactant−water interface when $w_0$ is as low as 2. In our model, $N_W$ does not exactly match the number of polar molecules, rather every particle represents (for example) a group of 2 or 3 water molecules. As noted above, a polar pool with $N_W$ = 4 (on average) forms a micelle of 18 surfactants. If we assume that each polar particle represents three water molecules, the lowest molar ratio between water and surfactant that guarantees the existence of a reverse micellar system is 0.7. Our results along with experimental studies[20,21] suggest that with $w_0 < 1$ ($w_0$ = 0.7 and 0.8 in ref 20 and ref 21, respectively) RMs can form, and therefore such pseudolattice structures may be dominant phases at the core. These findings encourage further atomistic simulations aimed at obtaining a quantitative measures on the RM aggregation number and the smallest possible size of the polar pool to have a permanent RM in a nonpolar solution.

Our findings show that, for $N_W/N_S > 0.5$, the shape of the RM is spherical, but this is not the case for lower ratios and even when there is no polar solvent in the solution. The largest aggregates have an elongated disk shape rather than a spherical shape, and it fluctuates over time thorugh the exchange of surfactant molecules with the solution. Recent atomistic simulations,[33,45] with preassembled spherical RMs have shown nonspherical shapes for RMs when the constraints are removed, and $w_0$ is as low as 3 and 6. Moreover, the final shape of an RM in atomistic simulations depends on the choice of the force field.[45] To interpret experimental results, a spherical geometry is assumed for RMs.[20] This assumption introduces errors in the calculation of aggregate sizes and other measures of RMs.

We show that the size of the polar core for $ht_6$ surfactants is smaller than the core for $ht_4$, as implied in Figure 9a. In other words, the polar solvent uptake by an RM decreases by increasing the length of the hydrocarbon tail. An experimental investigation has addressed this effect for fluorinated double-tail anionic surfactant/water/supercritical $CO_2$ microemulsions.[46] There is an increase in water uptake for smaller tails and a sharp decrease for larger tails, which gives an optimum tail length for the maximum uptake. The nonlinear behavior might be caused by oxyethylene spacer groups because the addition of more groups changes the overall trend. Both experimental methods and thermodynamic models with polar solvents can be applied to investigate this effect and further validate our results.

For micellar systems, the thermodynamic modeling has some superiorities over atomistic simulations: (i) There is no limit on the number of molecules used in the thermodynamic model. This is an issue with atomistic simulations particularly when



DOI: 10.1021/la504658u
Langmuir 2015, 31, 5982−5991

CMC is very low and one needs a large number of solvent molecules. Currently, it is not feasible to use atomistic simulations for CMC measurements in spite of the fact that this quantity is the most common measurement in micellar systems. Coarse-grained models can resolve this issue while structural details are compromised. (ii) The thermodynamic model gives a clear physical insight into how different free energies contribute to the micellization process. This leads to a better understanding of how the physical parameters of surfactants and solvents can influence CMC, aggregation number, and even the size distribution if it is implemented in the model. For this specific purpose, we need to develop a comprehensive thermodynamic model, which also includes polar solvents and their effects as suggested by our coarse-grained molecular dynamic simulations. Atomistic simulations in parallel with the thermodynamic model help to understand detailed structure of the RM core, specially when the number of polar molecules is very low. In this case, we expect that the counterions stay in close proximity of the ionic heads, and a pseudolattice structure forms with a dramatic reduction in mobility of all molecules in the core.

## AUTHOR INFORMATION


### Corresponding Author

*Phone: +1 (650) 3269172. Fax: +1 (650) 4729285. E-mail: abbas.firoozabadi@yale.edu.


### Notes

The authors declare no competing financial interest.

## ACKNOWLEDGMENTS

We are grateful to Boris Lukanov for helpful discussions and Mir Abbas Jalali for proof-reading of the manuscript. We thank the member companies of the Reservoir Engineering Research Institute (RERI) for their financial support.

## REFERENCES


(1) Moreira, L.; Firoozabadi, A. Molecular thermodynamic modeling of specific ion effects on micellization of ionic surfactants. *Langmuir* **2010**, *26*, 15177−15191.

(2) Lukanov, B.; Firoozabadi, A. Specific ion effects on the self-assembly of ionic surfactants: A molecular thermodynamic theory of micellization with dispersion forces. *Langmuir* **2014**, *30*, 6373−6383.

(3) Ruckenstein, E.; Nagarajan, R. Aggregation of amphiphiles in nonaqueous media. *J. Phys. Chem.* **1980**, *84*, 1349−1358.

(4) Eastoe, J.; Hollamby, M. J.; Hudson, L. Recent advances in nanoparticle synthesis with reversed micelles. *Adv. Colloid Interface Sci.* **2006**, *128*, 5−15.

(5) Silva, O. F.; Correa, N. M.; Silber, J. J.; de Rossi, R. H.; Fernandez, M. A. Supramolecular assemblies obtained by mixing different cyclodextrins and AOT or BHDC reverse micelles. *Langmuir* **2014**, *30*, 3354−3362.

(6) Klinkenberg, A., van der Minne, J. L., Shell, R. D. *Electrostatics in the Petroleum Industry: The Prevention of Explosion Hazards*; Elsevier Publishing Company: Amsterdam/New York, 1958.

(7) Leon, O.; Rogel, E.; Torres, G.; Lucas, A. Electrophoretic mobility and stabilization of asphaltenes in low conductivity media. *Pet. Sci. Technol.* **2000**, *18*, 913−927.

(8) Hsu, M. F.; Dufresne, E. R.; Weitz, D. A. Charge stabilization in nonpolar solvents. *Langmuir* **2005**, *21*, 4881−4887.

(9) Roberts, G. S.; Sanchez, R.; Kemp, R.; Wood, T.; Bartlett, P. Electrostatic charging of nonpolar colloids by reverse micelles. *Langmuir* **2008**, *24*, 6530−6541.

(10) Cummings, S.; Xing, D.; Enick, R.; Rogers, S.; Heenan, R.; Grillo, I.; Eastoe, J. Design principles for supercritical $CO_2$ viscosifiers. *Soft Matter* **2012**, *8*, 7044−7055.

(11) Jung, S.; Kim, J. H.; Kim, J.; Choi, S.; Lee, J.; Park, I.; Hyeon, T.; Kim, D.-H. Reverse-micelle-induced porous pressure-sensitive rubber for wearable human−machine interfaces. *Adv. Mater.* **2014**, *26*, 4825−4830.

(12) Suzuki, A.; Yui, H. Crystallization of confined water pools with radii greater than 1 nm in AOT reverse micelles. *Langmuir* **2014**, *30*, 7274−7282.

(13) Faeder, J.; Ladanyi, B. M. Solvation dynamics in reverse micelles: The role of headgroup−solute interactions. *J. Phys. Chem. B* **2005**, *109*, 6732−6740.

(14) Agazzi, F. M.; Correa, N. M.; Rodriguez, J. Molecular dynamics simulation of water/BHDC cationic reverse micelles. Structural characterization, dynamical properties and the influence of the solvent on the intermicellar interactions. *Langmuir* **2014**, *30*, 9643−9653.

(15) Zulauf, M.; Eicke, H. F. Inverted micelles and microemulsions in the ternary system water/aerosol−OT/isooctane as studied by photon correlation spectroscopy. *J. Phys. Chem.* **1979**, *83*, 480−486.

(16) Zhu, D.; Feng, K.; Schelly, Z. Reverse micelles of Triton X-100 in cyclohexane: Effects of temperature, water content, and salinity on the aggregation behavior. *J. Phys. Chem.* **1992**, *96*, 2382−2385.

(17) Correa, N. M.; Biasutti, M. A.; Silber, J. J. Micropolarity of reversed micelles: Comparison between anionic, cationic, and nonionic reversed micelles. *J. Colloid Interface Sci.* **1996**, *184*, 570−578.

(18) Sainis, S. K.; Merrill, J. W.; Dufresne, E. R. Electrostatic interactions of colloidal particles at vanishing ionic strength. *Langmuir* **2008**, *24*, 13334−13337.

(19) Biswas, R.; Rohman, N.; Pradhan, T.; Buchner, R. Intramolecular charge transfer reaction, polarity, and dielectric relaxation in AOTwaterheptane reverse micelles: Pool size dependence. *J. Phys. Chem. B* **2008**, *112*, 9379−9388.

(20) Kotlarchyk, M.; Huang, J. S.; Chen, S. H. Structure of AOT reversed micelles determined by small-angle neutron scattering. *J. Phys. Chem.* **1985**, *89*, 4382−4386.

(21) Smith, G. N.; Brown, P.; Rogers, S. E.; Eastoe, J. Evidence for a critical micelle concentration of surfactants in hydrocarbon solvents. *Langmuir* **2013**, *29*, 3252−3258.

(22) Falcone, R. D.; Silber, J. J.; Correa, N. M. What are the factors that control non-aqueous/AOT/n-heptane reverse micelle sizes? A dynamic light scattering study. *Phys. Chem. Chem. Phys.* **2009**, *11*, 11096−11100.

(23) Schatzberg, P. Solubilities of water in several normal alkanes from $C_7$ to $C_{16}$. *J. Phys. Chem.* **1963**, *67*, 776−779.

(24) Wing, J.; Johnston, W. The solubility of water in aromatic halides. *J. Am. Chem. Soc.* **1957**, *79*, 864−865.

(25) Aslan, S.; Firoozabadi, A. Effect of water on deposition, aggregate size, and viscosity of asphaltenes. *Langmuir* **2014**, *30*, 3658−3664.

(26) Goetz, R.; Lipowsky, R. Computer simulations of bilayer membranes: Self-assembly and interfacial tension. *J. Chem. Phys.* **1998**, *108*, 7397−7409.

(27) den Otter, W.; Shkulipa, S. Intermonolayer friction and surface shear viscosity of lipid bilayer membranes. *Biophys. J.* **2007**, *93*, 423−433.

(28) Khoshnood, A.; Noguchi, H.; Gompper, G. Lipid membranes with transmembrane proteins in shear flow. *J. Chem. Phys.* **2010**, *132*, 025101.

(29) Khoshnood, A.; Jalali, M. A. Anomalous diffusion of proteins in sheared lipid membranes. *Phys. Rev. E* **2013**, *88*, 032705.

(30) Bahrami, A. H.; Jalali, M. A. Vesicle deformations by clusters of transmembrane proteins. *J. Chem. Phys.* **2011**, *134*, 085106.

(31) Muller, N. Multiple-equilibrium model for the micellization of ionic surfactants in nonaqueous solvents. *J. Phys. Chem.* **1975**, *79*, 287−291.

(32) Muller, N. Attempt at a unified interpretation of the self-association of 1−1 ionic surfactants in solvents of low dielectric constant. *J. Colloid Interface Sci.* **1978**, *63*, 383−393.

(33) Vasquez, V.; Williams, B.; Graeve, O. Stability and comparative analysis of AOT/water/isooctane reverse micelle system using




DOI: 10.1021/la504658u
*Langmuir* 2015, 31, 5982−5991

dynamic light scattering and molecular dynamics. *J. Phys. Chem. B* **2011**, *115*, 2979−2987.
(34) Bondi, A. Free volumes and free rotation in simple liquids and liquid saturated hydrocarbons. *J. Phys. Chem.* **1954**, *58*, 929−939.
(35) Hildebrand, J. H., Prausnitz, J. M., Scott, R. L. *Regular and related solutions: The solubility of gases, liquids, and solids*; Van Nostrand Reinhold: New York, 1970.
(36) Zhou, J.; Tits, A.; Lawrence, C.User's Guide for FFSQP Version 3.7: A Fortran code for solving optimization programs, possibly minimax, with general inequality constraints and linear equality constraints, generating feasible iterates. *Technical Report SRC-TR-92−107r5*; Institute for Systems Research, University of Maryland: College Park, MD, 1997
(37) Assih, T.; Larche, F.; Delord, P. Evolution of the radius of the inverse micelles at high dilution in the aerosol-OT/Water/*n*-decane system. *J. Colloid Interface Sci.* **1982**, *89*, 35−39.
(38) Hellsing, M. S.; Rennie, A. R.; Hughes, A. V. Effect of concentration and addition of ions on the adsorption of aerosol-OT to sapphire. *Langmuir* **2010**, *26*, 14567−14573.
(39) Esumi, K., Ueno, M. *Structure−Performance Relationships in Surfactants*; CRC Press: Boca Raton, FL, 2003.
(40) Nyrkova, I.; Semenov, A. Multimerization: Closed or open association scenario? *Eur. Phys. J. E: Soft Matter Biol. Phys.* **2005**, *17*, 327−337.
(41) Blandamer, M. J.; Cullis, P. M.; Soldi, L. G.; Engberts, J. B.; Kacperska, A.; van Os, N. M.; Subha, M. Thermodynamics of micellar systems: Comparison of mass action and phase equilibrium models for the calculation of standard Gibbs energies of micelle formation. *Adv. Colloid Interface Sci.* **1995**, *58*, 171−209.
(42) Klíčóva, L.; Sebej, P.; Stacko, P.; Filippov, S. K.; Bogomolova, A.; Padilla, M.; Klan, P. CTAB/water/chloroform reverse micelles: A closed or open association model? *Langmuir* **2012**, *28*, 15185−15192.
(43) Southall, N. T.; Dill, K. A.; Haymet, A. A view of the hydrophobic effect. *J. Phys. Chem. B* **2002**, *106*, 521−533.
(44) Chowdhary, J.; Ladanyi, B. M. Molecular dynamics simulation of aerosol-OT reverse micelles. *J. Phys. Chem. B* **2009**, *113*, 15029−15039.
(45) Martinez, A. V.; Dominguez, L.; Małolepsza, E.; Moser, A.; Ziegler, Z.; Straub, J. E. Probing the structure and dynamics of confined water in AOT reverse micelles. *J. Phys. Chem. B* **2013**, *117*, 7345−7351.
(46) Sagisaka, M.; Koike, D.; Yoda, S.; Takebayashi, Y.; Furuya, T.; Yoshizawa, A.; Sakai, H.; Abe, M.; Otake, K. Optimum tail length of fluorinated double-tail anionic surfactant for water/supercritical $CO_2$ microemulsion formation. *Langmuir* **2007**, *23*, 8784−8788.



DOI: 10.1021/la504658u
*Langmuir* 2015, 31, 5982−5991